

Characterizing Respiratory Motion of the Major Abdominal Vessels

Ashley Gould Anderson III¹, Christopher François², and Oliver Wieben^{1,2}

¹Medical Physics, University of Wisconsin, Madison, Wisconsin, United States, ²Radiology, University of Wisconsin, Madison, Wisconsin, United States

Audience: Those interested in imaging abdominal vasculature.

Purpose: Free breathing acquisitions gated by bellows or navigators are appealing particularly for non-contrast enhanced MR angiography and 4D flow MRI as they extend the available imaging time beyond the limited durations of breath holds [1]. In order to optimize gating windows for such acquisitions, knowledge on the displacement and motion patterns of vessels in respect to the respiratory cycle is essential. Here we present a detailed analysis of the motion of 11 segments of major abdominal vessels (renal, hepatic, mesenteric, splenic arteries, aorta) during free breathing. In addition, vessel displacements during inspiration and expiration breath holds were measured in the same 10 volunteers. The results form a comprehensive reference for motion of the abdominal vasculature that extends the knowledge from previous motion studies.

Methods: Ten healthy subjects were imaged in a HIPAA-compliant, IRB-approved prospective study. A volumetric non-contrast-enhanced respiratory-gated MRA sequence (IFIR [2], Figure 1) served as a localizer for prescription of eight 2D slices to provide cross-sectional views through major abdominal vessels. Five sagittal slices captured anterior/posterior (AP) and superior/inferior (SI) motion of the proximal (1 cm from aorta) and distal (just before branching) renal arteries, the splenic artery, the common hepatic artery (CHA), and the origins of the celiac axis and the superior mesenteric artery (SMA). Three axial slices were placed to measure left/right (LR) and AP motion of the aorta at the level of the celiac/SMA, above the renal arteries, and above the iliac bifurcation. A near real-time (~3 fps) bSSFP sequence was used to acquire image series at each slice throughout several respiratory cycles (30-60 s). All scans were then repeated (frame rate reduced to 1 fps) during inspiration and expiration breath holds (9/10 subjects). Subjects were instructed to hold their breath as long as comfortable, up to 45 s. All acquisitions were performed on a clinical 3T scanner (MR HD750™, GE Healthcare, Waukesha, WI) with a 32-channel torso coil.

Vessel positions were tracked manually on the 2D image series. Free breathing measurements for each vessel were processed with a peak-detection algorithm to measure average vessel motion per breath. Standard deviations of the peaks and valleys of the total vessel displacement were calculated to provide a measure of end-expiration and end-inspiration position stability. Peak widths (within 2 mm of the detected maximum or minimum) were also measured to determine the ratio of total end-expiration to end-inspiration duration. Image quality was insufficient for tracking the celiac and SMA in one subject.

Results: Respiratory motion of the aorta was imperceptible at all three levels in all but one subject. Figure 2 shows the mean per-breath vessel motion for all other vessels for all ten subjects (nine subjects for celiac and SMA measurements). Error bars correspond to the group standard deviation. Table 1 shows the mean gating thresholds (respiratory efficiency) required to limit displacement to a given value for each vessel segment. The mean difference between end-expiration and end-inspiration stability for all measurements was 0.27 mm, which was found to be significantly lower ($p = 0.014$) using a one-tailed paired t-test. The period surrounding end-expiration was found to be 22% longer than that of end-inspiration.

Discussion and Conclusions: Figure 2 is arranged such that vessels near the aorta are in the center, with distal vessels near the edges of the plot. This data agrees with our and others' previous study of the renal arteries [3, 4], and shows distal vessels exhibit more total motion. These results also convey that respiratory motion in the abdomen is extremely non-rigid, and will be difficult to correct using most existing techniques. Surprisingly, significant motion (drift) was observed during inspiration and, to a lesser extent, expiration breath holds. This warrants further investigation of motion trends during breath holds. For longer scans, respiratory gating can reduce motion for all vessels to within the range of motion due to cardiac pulsatility, around 3 mm [5], with reasonable (>50%) efficiency (Table 1). Measures of end-expiration and end-inspiration duration and position stability confirm that restricting sampling to end-expiration is preferred for respiratory gating in the abdomen. Imaging in this phase should minimize artifact and maximize scan efficiency.

Acknowledgements: We gratefully acknowledge funding by NIH grant R01HL072260, and GE Healthcare for their assistance and support.

References:

- [1] R. L. Ehman, et al., *American Journal of Roentgenology*, 143(6): 1984, p.1175.
- [2] M. Katoh, et al., *Kidney International* 66(3): 2004, p. 1272.
- [3] A. G. Anderson III, et al., *17th Annual Meeting of ISMRM*: 2009, p. 3420.
- [4] M. T. Draney, *J. Endovascular Therapy* 12(3): 2005, p. 380.
- [5] D. W. Kaandorp, et al., *JMRI* 12(6): 2000, p. 924.

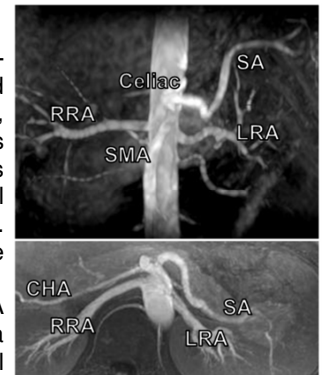


Figure 1 – Coronal (top) and axial (bottom) MIPs of the IFIR angiogram used for vessel localization.

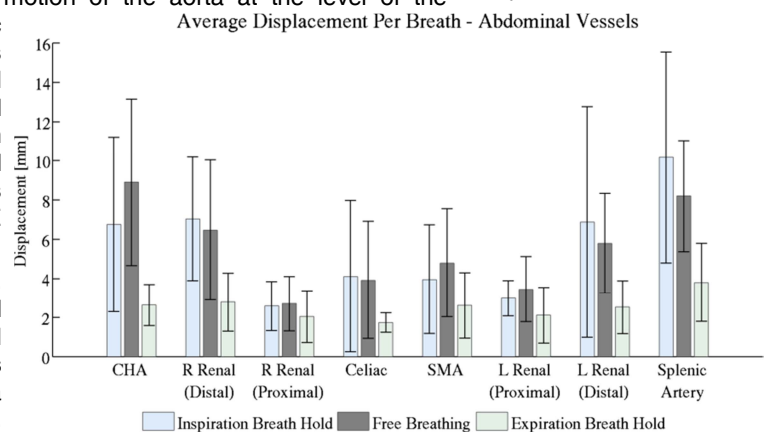


Figure 2 – Measured displacement of major abdominal vessels proximal (center) and distal (edges) to the aorta. Mean peak-to-peak displacement is shown for free breathing. Breath hold data represents drift during maximal breath holds (up to 45 s).

Table 1 – Mean data acceptance thresholds (corresponding to respiratory gating efficiency) required to limit motion of indicated vessels to within specified limits.

Maximum Displacement	CHA	R Renal (Distal)	R Renal (Proximal)	Celiac	SMA	L Renal (Proximal)	L Renal (Distal)	Splenic Artery
1 mm	25%	32%	52%	32%	34%	39%	37%	27%
2 mm	42%	52%	78%	60%	52%	65%	55%	44%
3 mm	53%	67%	89%	75%	67%	84%	68%	53%
4 mm	60%	76%	97%	87%	78%	90%	79%	61%
5 mm	68%	82%	99%	92%	88%	96%	87%	69%